AAS 11-548

ACHIEVABLE FORCE MODEL ACCURACIES FOR MESSENGER IN MERCURY ORBIT

Dale R. Stanbridge, Kenneth E. Williams, Anthony H. Taylor, Brian R. Page, Christopher G. Bryan, David W. Dunham, Peter Wolff, Bobby G. Williams*

and

James V. McAdams, Dawn P. Moessner †

The MErcury Surface, Space ENvironment, GEochemistry, and Ranging (MESSENGER) mission is the seventh mission in NASA's Discovery Program. The spacecraft, launched from Cape Canaveral Air Force Station in August 2004, arrived in orbit about Mercury in March 2011 to begin a one-year scientific investigation. While in orbit, the spacecraft is subject to a variety of forces, including Mercury and solar gravity, solar and planetary radiation effects, and propulsive events associated with orbit correction and momentum desaturation. This paper describes the challenges for navigation in terms of achieving the highest accuracy possible for relevant force models to support orbit determination and reconstruction over the Mercury orbital phase of the MESSENGER mission.

INTRODUCTION

The MErcury Surface, Space ENvironment, GEochemistry, and Ranging (MESSENGER) mission is being flown as the seventh mission in NASA's Discovery Program. Principal investigator, Sean C. Solomon of the Carnegie Institution of Washington, leads the MESSENGER mission. The Johns Hopkins University Applied Physics Laboratory (JHU/APL) designed and assembled the spacecraft and serves as the home for project management and spacecraft operations. Navigation for MESSENGER is provided by the Space Navigation and Flight Dynamics Practice of KinetX Aerospace Corporation.

While in orbit around Mercury, MESSENGER will continue to perform science observations of Mercury for at least one Earth year. The KinetX navigation team is responsible for processing NASA Deep Space Network (DSN) radiometric tracking data to produce the current and projected best estimate of the spacecraft trajectory for use in mission operations, science planning, and DSN tracking. The KinetX navigation team works closely with the mission design team at JHU/APL to validate and model the orbit-correction maneuvers (OCMs) that are periodically required to meet scientific objectives. KinetX uses the MIRAGE suite of software tools to perform high-precision orbit estimation and maneuver design validation for the MESSENGER spacecraft and other deep-space missions.

The MESSENGER navigation team is organized as part of a multi-mission navigation support group so that the team size can be adjusted as mission events dictate. Led by Ken

* All at KinetX Aerospace, Space Navigation and Flight Dynamics Practice, Simi Valley, California 93065.

† The Johns Hopkins University Applied Physics Laboratory, Laurel, Maryland 20723.

Williams, the MESSENGER navigation team is responsible for performing orbit determination (OD) for all phases of the mission. The JHU/APL mission design team has primary responsibility for OCM design and trajectory re-optimization in conjunction with the navigation team. OD for the orbit phase of the mission is based on the following DSN radiometric data types (abbreviations shown are standard DSN designations): two-way coherent Doppler (F2), three-way coherent Doppler (F3), and two-way ranging (SRA). Although delta differential one-way ranging (ΔDOR) was utilized during the mission cruise phase, it is not required for navigation while on orbit. Trajectories are predicted one month ahead to support operations and science planning. Predicted trajectories based on prior OD solutions are routinely compared with reconstructed (fit-span) trajectories to test the quality of previous orbit solutions and force modeling. These "radio-only" solutions are used to estimate the spacecraft state vector and certain dynamic parameters so that the classical elements and their uncertainties may be used to plan OCMs that are periodically required to correct the trajectory to meet the requirements of science planning.

As of this writing, MESSENGER has completed one Earth flyby, two Venus flybys, three Mercury flybys, and approximately one third of the first year on orbit at Mercury. Over the course of the mission, accurate orbit determination solutions have enabled the optimization of the trajectory and the planning of five deterministic deep-space maneuvers (DSMs), numerous statistical trajectory-correction maneuvers (TCMs), the Mercury orbit insertion (MOI) maneuver, and the first orbit-correction maneuver (OCM-1). Combined with trajectory re-optimizations after all trajectory corrections and high accuracy maneuver execution by the spacecraft and guidance and control (G&C) teams, the MESSENGER spacecraft has arrived at Mercury with sufficient fuel for the primary one-year orbital mission phase and a potential extended mission. The planning and execution of the MOI maneuver was extremely accurate for such a large trajectory change. Table 1 shows the results of the MOI reconstruction and the resultant classical elements for the initial Mercury orbit, relative to the Mercury true equator.

Table 1. MOI Targeted and Actual Orbit Parameters

Parameter	Reconstructed Value*	Target Value	Difference
Δv [m/s]	861.714	862.166	-0.452
Orbital Period [s]	43456.86	43195.48	261.38
Eccentricity	$0.740 \pm 9.44 \times 10^{-5}$	0.740	0.00038
Inclination [deg]	$82.52 \pm 4.90 \times 10^{-3}$	82.5	0.0219
RA of Asc Node [deg]	$350.17 \pm 2.26 \times 10^{-3}$	350.17	-0.0039
Periapsis Arg [deg]	$119.16 \pm 3.41 \times 10^{-3}$	119.13	0.034
Periapsis Lat [deg]	59.976	60.0	-0.024

* ± values are 3-standard-deviation formal uncertainties.

In what follows we discuss the preparations that were required by the navigation team to transition from cruise to orbit phase following MOI, the ongoing challenges that have been faced by the navigation team to improve the force models needed for accurate on-orbit trajectory estimation and prediction, and remaining challenges yet to be addressed for the one-year orbit phase. We discuss the orbit geometry and force-modeling environment in which MESSENGER operates while on orbit, and we describe the modeling used in the OD solutions. Uncertainties obtained from covariance analyses performed prior to arrival at Mercury are compared with preliminary reconstruction of the actual trajectories in the data fit span. The accuracy of the pre-orbit-phase Mercury modeling parameters will be discussed, with the benefit of several months of on-orbit data. Preliminary results of improved models obtained from on-orbit data provide a basis for planning of future work. Discussions of the navigation team's role during cruise, Mercury flybys, and MOI targeting are provided in related papers. [1, 2, 3]

Orbital Geometry and Environment

To help understand the dynamics, it is useful to visualize the MESSENGER orbit in the ecliptic frame, and the rotation of Mercury underneath. The MESSENGER orbit plane is nearly perpendicular to the ecliptic plane ($87.4° < i < 88.4°$ thus far) and lies approximately in the ecliptic x-z plane ($355° < \Omega < 360°$ thus far), where z is normal to the ecliptic plane, i is the inclination to the ecliptic plane, and Ω is the right ascension of the ascending node, also relative to the ecliptic plane. The periapsis argument varies from 114° at the beginning of the orbit phase down to 99° at the end of the one-year nominal mission. The Mercury spin axis has an ecliptic declination of 83°. Thus, the plane of the orbit is relatively stable in inertial space, with Mercury rotating once every 58.65 days underneath the orbit plane. Periapsis occurs over all longitudes of Mercury, but over a narrow range of northerly latitudes. Figure 1 shows an example of the orbital geometry, with ticks along the orbit every hour (the yellow line is the terminator). The nominal orbital period is 12 hours, but this period tends to decrease gradually as periapsis altitude increases due to solar gravity perturbations.

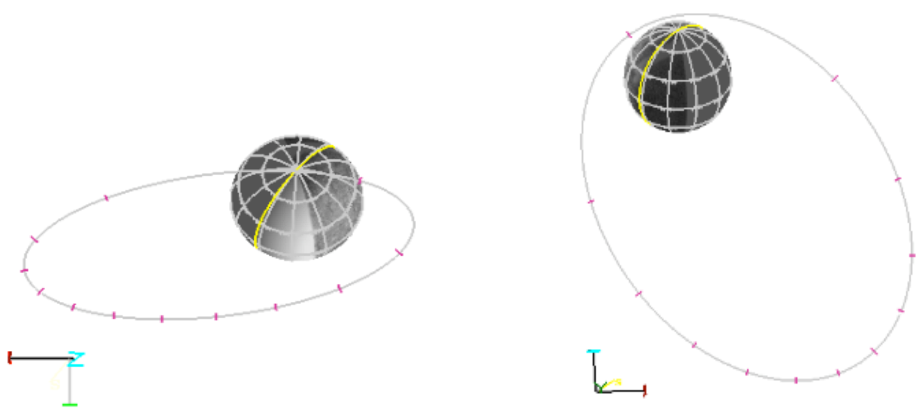

(a) Ecliptic x-y plane, +z out of page (b) Ecliptic x-z plane, +y into page

Figure 1. MESSENGER Orbit Plane Geometry.

Monthly snapshots, looking down from the ecliptic north pole, of the orbital geometry of Mercury, Earth, and Sun are shown in Figure 2. One can also see from this plot the seasons when the spacecraft passes behind Mercury's shadow. Earth is the blue outer dot, and Mercury is the gray dot. The line through Mercury represents the MESSENGER orbit plane. Also note that the orientation of the orbit plane varies with respect to the Earth-Mercury line, which tends to reduce line-of-sight observability for radiometric data when the orbit plane is normal to the Earth direction. The quality of the radiometric data is degraded for superior solar conjunctions, which occur when Earth and the spacecraft on opposite sides of the Sun and the angle between the Earth-Sun and Earth-spacecraft lines of sight, the Sun-Earth-probe (SEP) angle, falls within 10°.

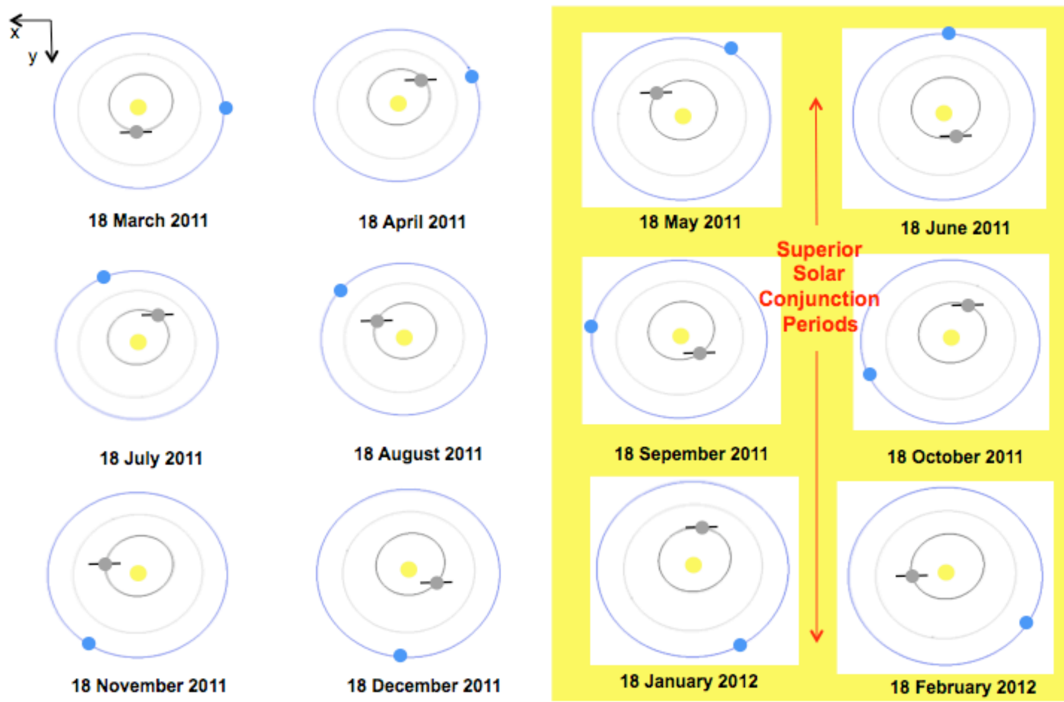

Figure 2. Earth Viewing Geometry for the Year in Orbit, Viewed from Ecliptic North. Periapsis is on the -X Side.

From Figure 1 and Figure 2, one can make the following observations. Because periapsis occurs at northerly latitudes and the orbit is highly eccentric, the resolution of the higher-order terms of the gravitational field will be better at northern latitudes and will be reduced somewhat over the southern half of the planet. The MESSENGER spacecraft will pass over the different regions of Mercury during different seasons. For instance, periapsis will sometimes occur on the dayside, and other times on the nightside, with the longitude of periapsis varying simultaneously. These effects may facilitate the separation of the albedo, infrared, and gravitational accelerations in the OD filter. Since they also vary as the inverse square of the distance, all these forces will be notably stronger near periapsis, but the albedo acceleration will be negligible when periapsis is over the nightside far from the terminator.

An additional challenge arises from the requirement that the spacecraft sunshade must be pointed at the Sun and the science instrumentation generally pointed at Mercury. These constraints require the spacecraft to rotate near each periapsis. This rotation, and the associated movement of the spacecraft antennas, alters slightly the frequency of the signal received from the spacecraft. The navigation team corrects for this effect in the Doppler tracking data by subtracting the line-of-sight antenna angular velocity from the received frequency. This correction requires accurate, high-resolution knowledge of the spacecraft attitude and is a potential source of error in the OD process. That this effect occurs mostly at periapsis, when the perturbations from the higher-order gravity terms have their strongest effect, poses additional challenges to the OD process.

Orbit Determination Strategy

The primary objectives of the MESSENGER navigation team are to determine the current and predicted spacecraft trajectory about Mercury with sufficient accuracy to meet scientific and operations requirements, and to be able to reconstruct the trajectories of the spacecraft about Mercury and Mercury about the Sun.

To achieve these objectives, approximately 10 hours per day of two-way and three-way Doppler data, along with ranging data, are used in the OD solutions. The sigma used for data weighting is nominally 0.5 mm/s for the Doppler data and 75 m for the range data. The Doppler data are compressed to 60-s density for normal OD operations, and the range data are typically acquired at 10-min intervals.

Superior solar conjunctions occur several times per year. The Doppler and ranging data signals can be degraded markedly as they pass through the solar plasma. During such periods, the tracking data weights are adjusted to reflect the increased noise, according to an empirical scheme derived from previous observations of the pass-by-pass noise. Doppler weighting is generally set according to the inverse square of the expected one-sigma noise level. Range data during solar conjunction periods are weighted at around 1 km for SEP angles less than 4°, and about 300 m for SEP angles between 4 and 10°. Figure 3 shows the expected Doppler noise level during a solar conjunction period.

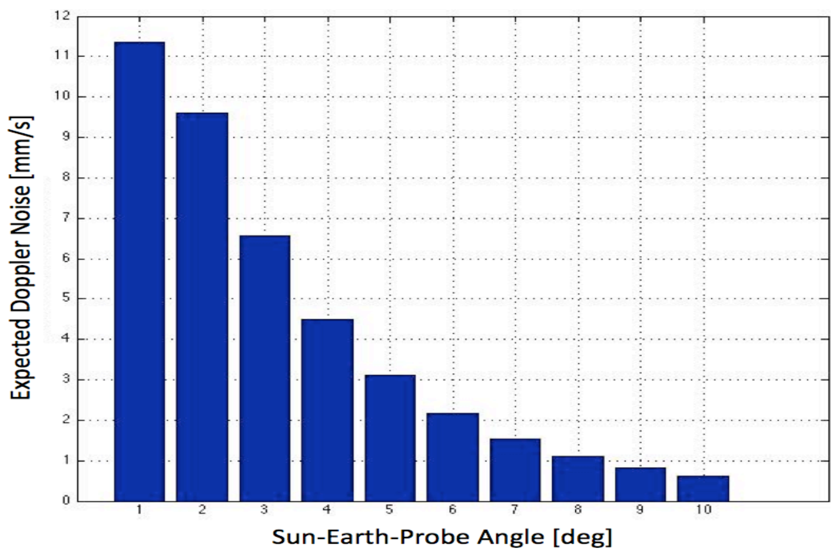

Figure 3. Expected Doppler Noise Level During Solar Conjunction.

The navigation team typically delivers an OD solution and corresponding trajectory once per week. Data arcs are approximately nine days long, beginning at the apoapsis nearest 20:00 UTC on Monday, with a tracking data cutoff at 20:00 UTC on Wednesdays. The project typically performs commanded angular momentum dumps weekly on Tuesdays, so there is generally one to two in the fit span. The predicted trajectory generated and delivered to the project runs 30-35 days after the tracking data cutoff to support near-term science sequence planning. There is no a priori knowledge of the magnitude and direction of the future commanded momentum dumps, so they cannot be included as perturbations in the predicted trajectory. This predicted trajectory is used for DSN tracking and for the planning of observations and instrument pointing by the science team. A nominal OD timeline is shown in Figure 4.

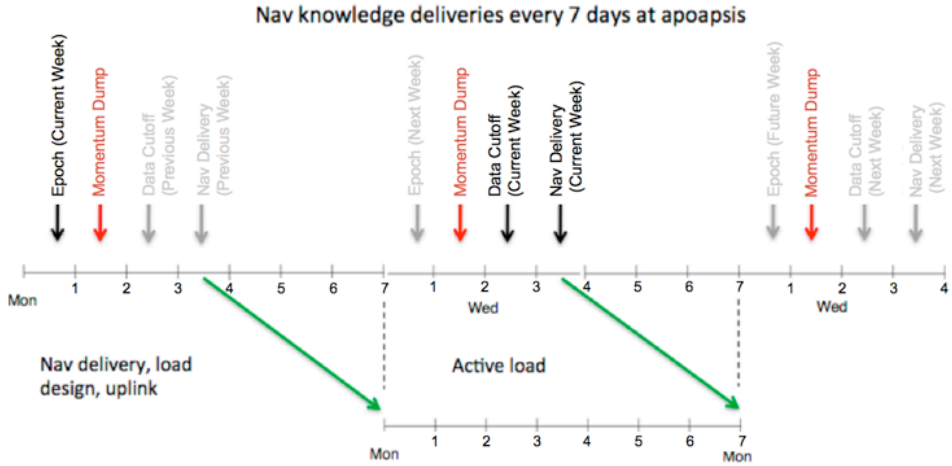

Figure 4. Nominal OD Timeline.

Orbit determination calls for accurate physical models describing the forces acting on the spacecraft. The dominant forces include Mercury and solar gravity, solar radiation pressure (SRP), planetary radiation pressure (PRP) from the Sun reflected off of the planet surface and back to the spacecraft (albedo reflection), and infrared (IR) or thermal radiation from Mercury. Table 2 shows an example solution with the relative magnitudes of the accelerations acting on MESSENGER at periapsis (altitude 207 km) for an early operational delivery.

Table 2. Accelerations Acting on MESSENGER at Periapsis

Acceleration Source	Approximate Magnitude [km/s^2]
Central Force (due to GM)	3×10^{-3}
Gravitational Harmonics (J_2 and above)	5×10^{-7}
Solar Gravitation	4×10^{-9}
Solar Radiation Pressure	7×10^{-10}
Thermal Planetary Radiation	2×10^{-11}
Reflected Planetary Radiation (Albedo)	6×10^{-12}

The estimated and considered parameters in the OD filter are given in Table 3.

Table 3. Estimated and Considered Parameters

Estimated Parameters	Considered Parameters
Position / Velocity	Station Locations
SRP Reflectivity Coefficients	Troposphere Model Parameters
Albedo Reflectivity Coefficients	Ionosphere Model Parameters
Infrared Reflectivity Coefficients	Earth Pole, UT1
Commanded Momentum Dumps	Earth Ephemeris
Orbit Correction Maneuvers	
Mercury Ephemeris	
Mercury Gravity	

The a priori Mercury ephemeris used initially in Mercury orbit is the DE423 planetary ephemeris, produced by the Jet Propulsion Laboratory (JPL) Solar System Dynamics Group specifically for the MESSENGER project. It is based on data provided by the navigation team for the three Mercury flybys. The Mercury Sun-centered ephemeris state is estimated as part of the OD process.

Arrival and Initial Orbit Determination in Mercury Orbit

Upon MESSENGER's arrival at Mercury, it was immediately evident that there was dynamic mismodeling in the OD filter, as was expected given the limited data available before orbit insertion. The tracking data were very difficult to fit, and estimated model parameters often ill behaved, with marked aliasing between parameters. In particular, the converged Doppler residuals showed a non-random "tail" signature around periapsis, and there was a tendency for the IR and albedo reflectivity coefficients to go negative, which is not physically realistic. Figure 5 shows an example of the Doppler and ranging residuals of an early solution while in orbit (scale is mm/s and meters respectively).

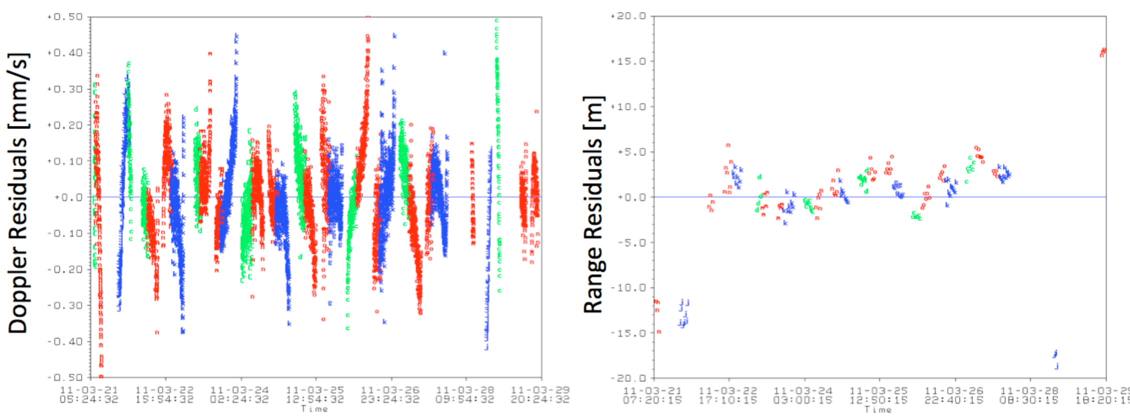

(a) Doppler

(b) Range

Figure 5. Early Example of (a) Doppler, and (b) Range OD Residuals.

In order to gain some insight into the nature of the dynamic mismodeling at periapsis, the navigation team performed an experiment just after MOI, which consisted of modeling a hypothetical impulsive maneuver at each periapsis. The nominal value for the maneuver Δv was zero, but the filter was provided a 1-standard-deviation (1-σ) a priori uncertainty of 100 mm/s. The experiment yielded a much better fit to the data, with an average solved-for pseudo maneuver magnitude of 17 mm/s. Another interesting by-product of adding this pseudo maneuver was that it was not necessary to overly constrain the IR and albedo a priori uncertainties in order to fit the data. Figure 6 shows the residuals obtained.

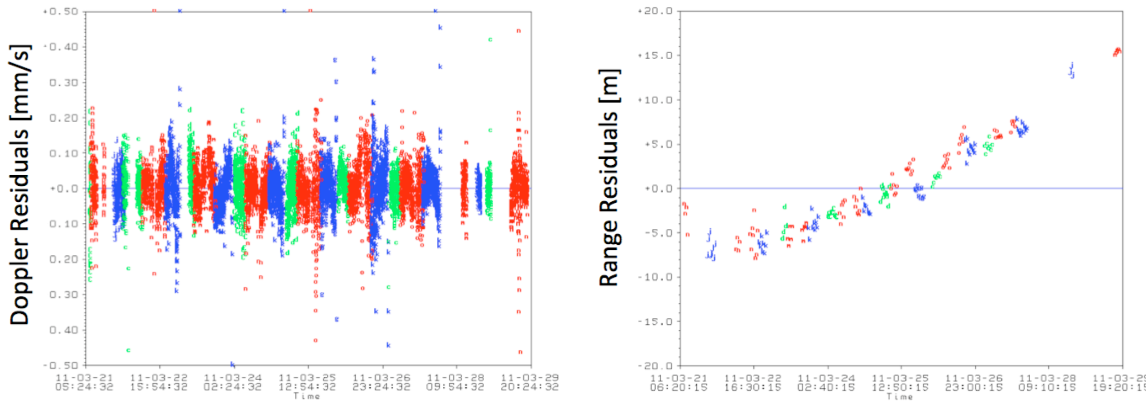

(a) Doppler (b) Range

Figure 6. Doppler (a) and Range (b) OD Residuals after Estimating an Impulsive Maneuver at Periapsis.

It was apparent from the solved-for pseudo maneuver magnitudes that there was a discernable pattern, but that it was not sufficiently consistent over time to form any simple conclusions, or to be able to use this information in a propagation beyond the fit span. Figure 7 shows the resultant Δv's (scale is mm/s) for the solved-for pseudo maneuvers in the UVW frame, where U is directed along the position vector, W is directed along the orbit normal, and V completes the right handed set. Apparently, un-modeled forces near periapsis could be approximated by impulsive maneuvers to first order, but only for analysis purposes. These results suggested a need for updated force models in the orbit determination setup.

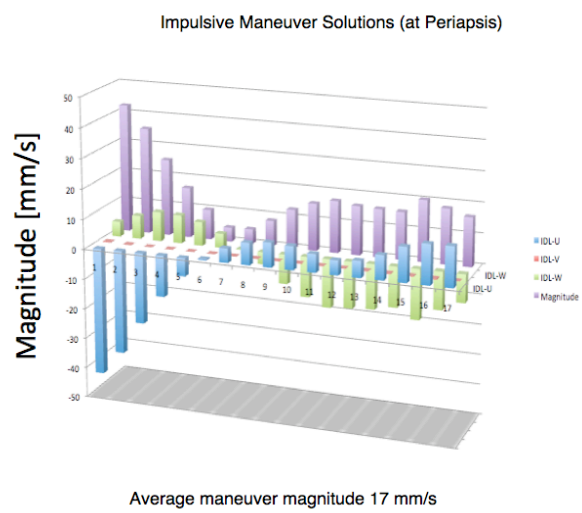

	Impulsive Maneuver (mm/s)			
Date/Time	IDL-U	IDL-V	IDL-W	Magnitude
21-MAR-2011 13:19:13 ET	-42.250	0.158	5.045	42.550
22-MAR-2011 01:23:32 ET	-34.390	-0.024	7.767	35.257
22-MAR-2011 13:27:53 ET	-23.511	0.004	9.666	25.421
23-MAR-2011 01:32:13 ET	-13.713	-0.025	9.393	16.622
23-MAR-2011 13:36:35 ET	-5.969	-0.014	7.820	9.838
24-MAR-2011 01:40:57 ET	0.414	-0.038	4.588	4.607
24-MAR-2011 13:45:19 ET	4.776	-0.035	0.211	4.781
25-MAR-2011 01:49:42 ET	7.349	-0.057	-4.095	8.413
25-MAR-2011 13:54:05 ET	8.198	-0.066	-9.749	12.738
26-MAR-2011 01:58:28 ET	7.833	-0.081	-13.387	15.510
26-MAR-2011 14:02:52 ET	6.078	-0.087	-15.962	17.080
27-MAR-2011 02:07:16 ET	4.761	-0.083	-15.372	16.092
27-MAR-2011 14:11:41 ET	5.428	-0.084	-14.860	15.820
28-MAR-2011 02:16:05 ET	8.078	-0.113	-13.382	15.632
28-MAR-2011 14:20:30 ET	11.489	-0.100	-16.679	20.254
29-MAR-2011 02:24:55 ET	13.160	-0.269	-12.516	18.163
29-MAR-2011 14:29:19 ET	13.229	0.011	-9.312	16.178

Figure 7. Resultant Pseudo Maneuver at Periapsis Results in UVW-Frame.

Mercury A Priori Physical Models – Orientation, Gravity, Planetary Radiation Pressure

Mercury Orientation

The orientation model used for MESSENGER navigation is based on International Astronomical Union (IAU) conventions and other values compiled by Margot.[4] It uses three Euler angles to describe the orientation of the coordinate axes with respect to the inertial International Celestial Reference Frame (ICRF), where the fundamental plane is the Earth mean equator of J2000 (EME2000). The model provides for the right ascension (α) and declination (δ) of the Mercury pole, and the angle of the ascending node of the Mercury equator on the EME2000 *x-y* plane to the Mercury prime meridian (W). The formulation is:

$$
\begin{aligned}
\alpha &= 281.0097 - 0.0328T \\
\delta &= 61.4143 - 0.0049T \\
W &= 329.75 + 6.1385025d + Q(d) \\
Q(d) &= \\
&\quad 0.00993822\sin(174.791086 + 4.092335d) \\
&- 0.00104581\sin(349.582171 + 8.184670d) \\
&- 0.00010280\sin(164.373257 + 12.277005d) \\
&- 0.00002364\sin(339.164343 + 16.369340d) \\
&- 0.00000532\sin(153.955429 + 20.461675d)
\end{aligned}
\tag{1}
$$

where

d is the interval in days (of 86400 SI seconds) from J2000, and
T is the interval in Julian centuries (of 36525 days) from J2000.

Only the linear term in W is modeled in MIRAGE. This introduces an error of approximately 430 meters (0.01°) at Mercury's surface. Considering that the smallest longitude span of a spherical harmonic gravity model to degree and order 20 is 9°, which is approximately 380 km at Mercury's surface, this level of error is judged to be acceptable. For the determination of an operational gravity model used for navigation, this difference is not significant when only radiometric data are used. When optical data are introduced, however, where a one-pixel resolution at 200 km altitude amounts to about 5 m at the surface, this error could be as large as 84 pixels, which is significant. Optical data may be incorporated in a final reconstruction of the spacecraft trajectory for the entire Mercury orbital portion of the MESSENGER mission.

Gravitational Potential of Mercury

Prior to the MESSENGER MOI, there had been six prior flybys of Mercury, three by Mariner 10 in 1974 and 1975, and three by MESSENGER in 2008 and 2009. These flybys provided the basis for the a priori Mercury gravity model. Table 4 gives a summary of these flybys.

Table 4. Mariner 10 and MESSENGER Flybys

Description	Periapsis Altitude	Comments
Mariner 10, 29 March 1974	706 km	Equatorial (-1.7° lat, occulted)
Mariner 10, 21 September 1974	48,069 km	Southern
Mariner 10, 16 March 1975	327 km	Northern (67.6° lat)
MESSENGER, 16 January 2008	201 km	Southern (near equator)
MESSENGER, 6 October 2008	199 km	Southern (near equator)
MESSENGER, 29 September 2009	227 km	Southern (near equator)

To determine an a priori Mercury gravitational model for MOI and early orbit phase, we used a method implemented by A. H. Taylor of the MESSENGER navigation team based on square root information (SRI) filter theory, as described by Bierman.[5] As illustrated in Figure 8, this method entails constructing a set of data equations $Rdx = dz$ in SRI filter format for each data arc (typically 7 days in length). These data equations are modified to collect gravity parameters at the end and triangularized. The non-gravity portion of the data equations for each arc is discarded, and the remaining gravity portions are adjoined into a single triangular array and solved by back substitution to obtain a combined solution. R is the SRI matrix (upper triangular), dz is the solution residual vector, and dx is the solution vector.

The method depends on starting with a gravity a priori data equation with new data obtained from the OD process in which no a priori information about gravity parameters is included. The a priori data equation used by the navigation team was obtained from Mariner 10 flybys.[6] Estimated Mariner 10 values of the product of the gravitational constant and Mercury's mass GM and the second-degree zonal and tesseral coefficients in the gravitational potential, J_2 and C_{22}, were normalized and truncated to obtain[6,7]

$$\begin{aligned} GM &= 22032.09 \pm 0.91 \ km^3 \sec^{-2}, \\ J_2 &= 2.7 \times 10^{-5}, \\ C_{22} &= 1.6 \times 10^{-5}. \end{aligned}$$

The a priori uncertainties follow Kaula's rule[8], as suggested by Smith[7] of $80 \mathrm{x} 10^{-6}/n^2$, where n is the degree, except for the harmonic coefficients C_{21} and S_{21}, for which smaller a priori uncertainties were used to constrain the values close to zero. The a priori equation is then combined with other data equations from the OD process to produce a final data equation, which is solved to produce the estimated gravity parameters and covariance.

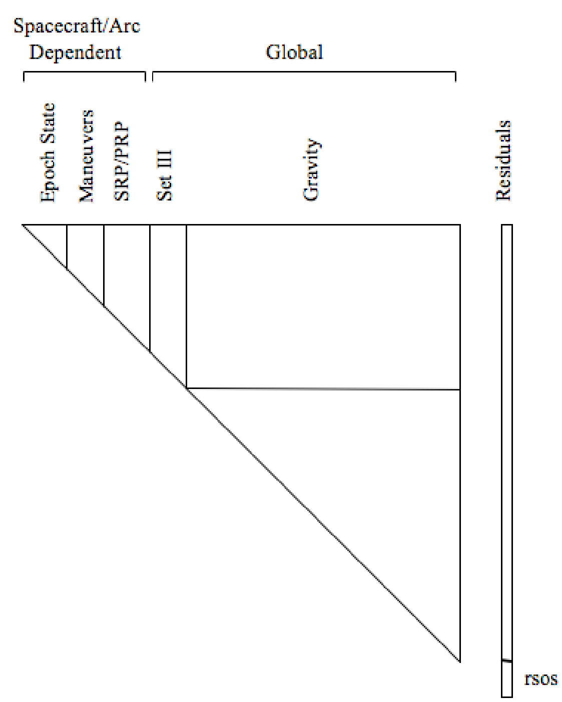

Figure 8. SRI Gravity Combination Scheme.

The best current estimate of the gravitational harmonics is obtained from back substitution as

$$x = R^{-1} z . \tag{2}$$

The solution vector x is obtained from $x = x$ (nominal) + dx, after a "leveling" process is applied that adjusts the residual vectors for a common (globally applicable) set of nominal values.

The covariance matrix is obtained as

$$P = \left(R^T R\right)^{-1} . \tag{3}$$

Figure 9 shows qualitative results of the evolution of gravitational surface potentials and associated uncertainties derived from this data. The left column shows a priori information obtained from Mariner 10, and the right column includes both Mariner 10 and MESSENGER flybys 1-3.

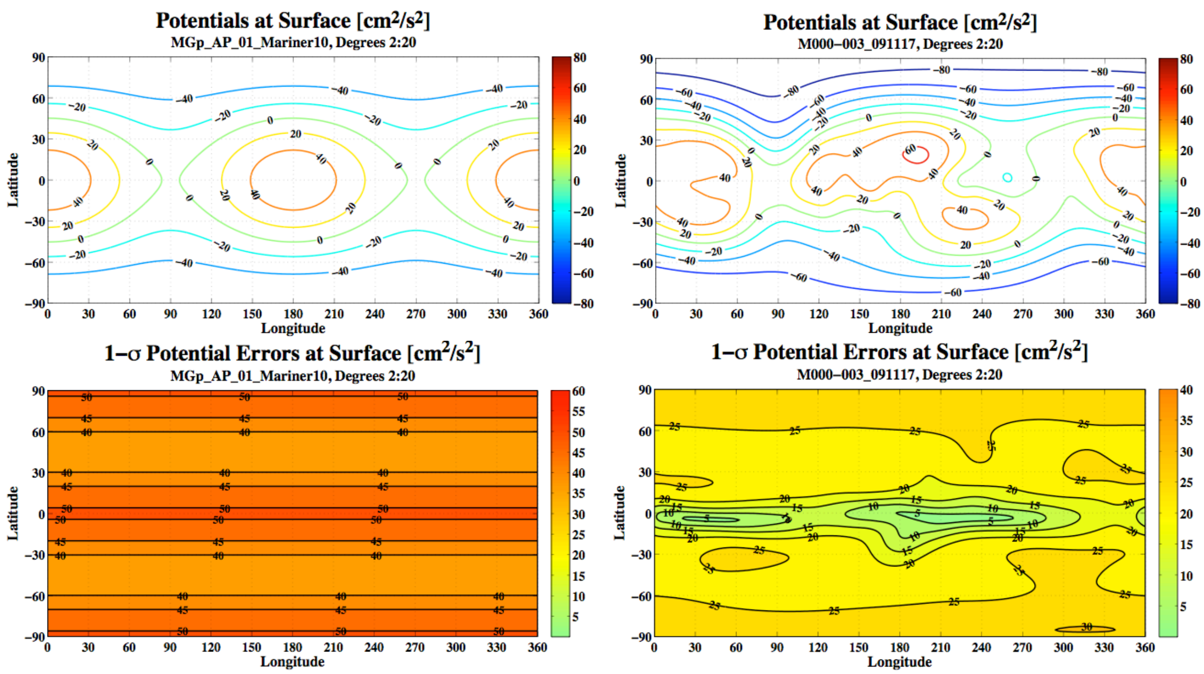

(a) Mariner 10 a priori (b) Mariner 10 and MESSENGER flybys 1-3

Figure 9. Evolution of the Mercury Gravitational Potential for Mariner 10 and MESSENGER Flybys 1-3.

An updated 20 × 20 gravitational model for use by the navigation team, developed by A. H. Taylor, incorporates several weeks of orbital data. This model was tested on the data arcs with data cutoffs of 6 and 13 April 2011. It was found that the updated gravity model significantly improved the fit to the data. Convergence was easier and the behavior of the planetary radiation pressure reflectivity coefficients was improved, without the previous tendency of the filter to make some parameters physically unrealistic. This information has been provided to the MESSENGER radio science team as part of the effort to obtain the most definitive estimate of the Mercury gravity field.

A comparison of the post-fit Doppler and range residuals, using an initial 10 × 10 and an updated 20 × 20 gravitational model in an operational OD solution, is shown in Figure 10. Improvement in the residuals is evident in the 20 x 20 case.

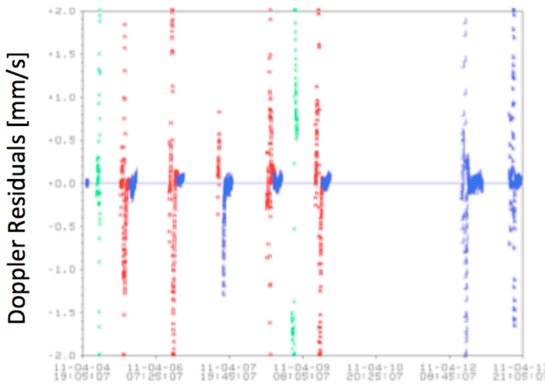

(a) Doppler

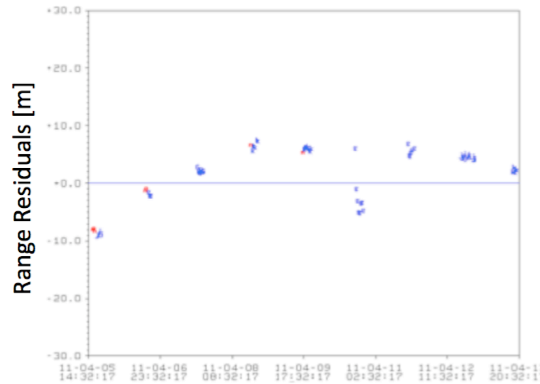

(b) Range

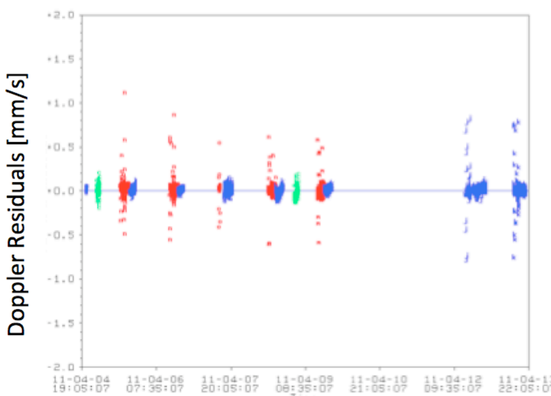

(c) Doppler

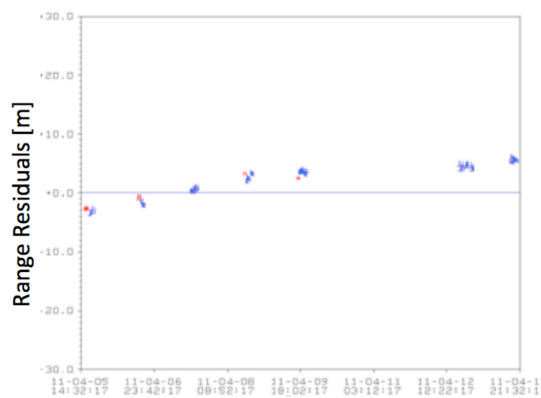

(d) Range

Figure 10. Post-fit Doppler and Ranging Residuals Using (a, b) 10×10 A Priori Gravity Model, and (c, d) 20×20 A Priori Gravity Model.

Planetary Radiation Pressure Modeling

A priori models for the acceleration exerted on a spacecraft by the radiation coming from Mercury were based on the work of Borderies et al.[9, 10] General models were developed for both the radiation reflected by the planet onto the spacecraft, albedo, and the infrared thermal emission (IR) associated with its temperature. Both albedo and IR are modeled as spherical harmonics with respect to the Mercury IAU reference frame. Borderies assumed a spacecraft model consisting of a "juxtaposition of planar surfaces," which is consistent with the MESSENGER navigation spacecraft model. A challenge for the navigation team was to devise with an initial model using the framework of Borderies.

An empirical Mercury IR model was developed from models of Mercury surface temperature variations measured or postulated in support of the BepiColombo mission.[11]. Subsolar temperature was modeled as a function of Mercury-Sun distance, as shown in Figure 11. In addition, temperature variations were provided at a fixed longitude at Mercury-fixed latitudes of 0°, 65°, and 85° over one Mercury solar day (approximately 176 Earth days), thus covering a full range of Sun-relative longitudes. Data corresponding to perihelion (Figure 12a) and aphelion (Figure 12b) conditions were extracted from the data sets provided.

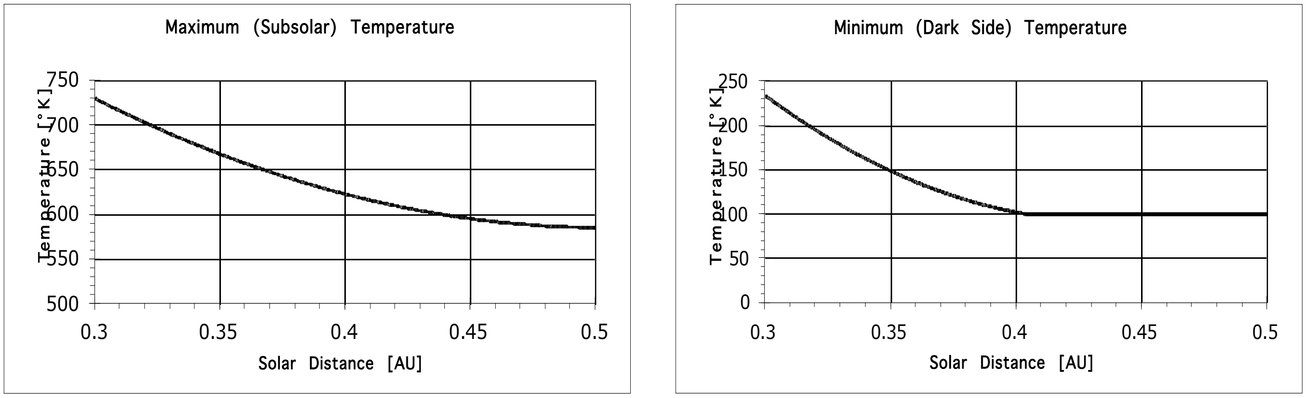

(a) Maximum Subsolar Temperature (b) Minimum Subsolar Temperature

Figure 11. Subsolar Temperature Model Postulated for BepiColombo.

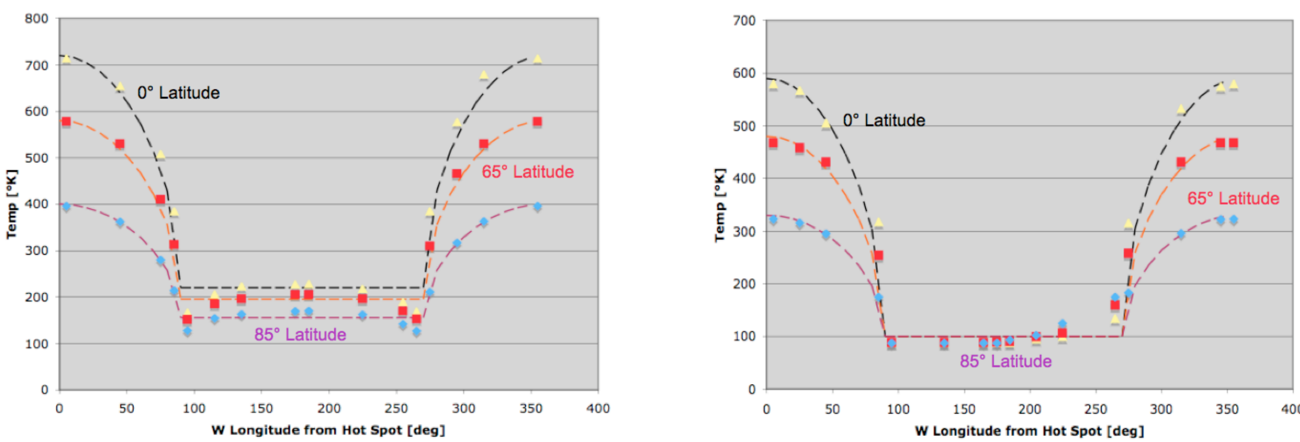

(a) Perihelion (b) Aphelion

Figure 12. Temperature Data Extracted for Perihelion (Days 0 and 88) and Aphelion (Days 44 and 132) Conditions.

Data in Figure 12 could be fit approximately by functions having the following form:

$$T = T_{\min} + (T_{\max}\text{-}T_{\min})*(\cos\theta)^{1/3}, \qquad \theta < 90° \text{ or } \theta > 270°,$$

$$T \sim T_{\min}, \qquad \theta \geq 90° \text{ and } \theta \leq 270°. \qquad (4)$$

where

$T_{\min}$ is a minimum temperature representing the average temperature on Mercury's nightside,
$T_{\max}$ is a maximum temperature at the subsolar point, and
θ is the longitude relative to the subsolar point.

These relationships can be generalized to cover a full range of latitudes by replacing θ by angular radius ρ, yielding

$$T = T_{\min} + (T_{\max}\text{-}T_{\min})*(\cos\rho)^{1/3}, \qquad \rho < 90° \text{ or } \rho > 270°,$$

$$T \sim T_{\min}, \qquad \rho \geq 90° \text{ and } \rho \leq 270°. \qquad (5)$$

Minimum and maximum temperatures are selected on the basis of values derived from Figure 11, a representative sample of which is shown in Table 5, from which a range of values can be interpolated.

Table 5. Selected Minimum and Maximum Temperatures as Functions of Mercury Solar Distance.

Solar Distance [AU]	Solar Distance [10^6 km]	Max. Temp [K]	Min. Temp [K]
0.467	69.9	590	100
0.404	60.4	620	100
0.307	45.9	720	220

Because the temperature distribution defined above is tied to the surface of Mercury which slowly rotates below the orbit of the MESSENGER spacecraft, a new distribution must be defined for mean conditions covering periods 7-10 days in duration over which the radiometric OD filter is applied. The actual distribution provided to the navigation software is in the form of emissive power E, which is defined in terms of spherical harmonic coefficients. For a given Mercury-Sun-spacecraft geometry, a set of spherical harmonics to degree and order 10 are derived from a grid of T^4, in accordance with the Stefan-Boltzmann equation, where T is as specified above for each data point. The overall scaling applied to E, as well as diffuse and specular reflectivities, are estimated as dynamic parameters in the OD filter.

The resultant accelerations form the basis for the a priori planetary radiation pressure models. They are modeled in the OD process, and the specular and diffuse reflectivity coefficients are the dynamic parameters whose values are estimated in the OD filter.

Spacecraft Reflectivity Model

For the purposes of modeling the forces due to radiation pressure, the spacecraft is approximated as 10 flat plates. Specular and diffuse reflectivity coefficients are the parameters in to be determined in the SRP, planetary infrared, and albedo models. These plates are defined as follows, in spacecraft coordinates[12]:

Table 6. Spacecraft SRP Plate Definitions.

Plate	Description
1. –X side of sunshade	0.836 x 2.538 m^2
2. Center of sunshade, along –Y	0.498 x 2.538 m^2
3. +X side of sunshade	0.836 x 2.538 m^2
4. ± X side of the spacecraft	Nominally doesn’t see the Sun
5. ± Z side of the spacecraft	Nominally doesn’t see the Sun
6. +Y (back) side of the spacecraft	1.817 x 2.538 m^2
7. Front side of –X solar panel	2.724 m^2
8. Front side of +X solar panel	2.724 m^2
9. Back side of –X solar panel	2.724 m^2
10. Back side of +X solar panel	2.724 m^2

Covariance Analysis

Prior to MOI, covariance analyses were performed by the navigation team using the planned tracking schedule for different phases of the orbit. The objective was to determine the contribution to the predicted position/velocity OD errors due to uncertainties of the OCMs, commanded momentum dumps, solar panel angle mismodeling, and whether the OD estimates might benefit from the use of ΔDOR data (particularly when the orbit plane is in the plane of the sky as seen from Earth). Also, the effects of the various seasons and range of periapsis altitudes were examined.

As shown in the nominal OD timeline (Figure 4), the epoch is chosen near the second apoapsis on each Monday. The data arc is approximately 9 days long, with a tracking data cutoff on Wednesdays at 20:00 UTC. The covariance analysis assumed that there is a commanded momentum dump every Tuesday with a zero nominal magnitude, but with a spherical uncertainty of 1.4 mm/s. After data cutoff (DCO), the trajectory is propagated out for ~30 days, and the uncertainties are mapped forward throughout the prediction span. Of particular interest were the uncertainties in the radial, transverse (along-track), normal (RTN) frame. Due to coupling between the radial and transverse directions, the uncertainties of most interest were the radius of periapsis and the time from periapsis.

It was found that the predicted OD uncertainties were dominated by the uncertainty associated with the unmodeled commanded momentum dumps. Momentum dumps that are modeled and solved-for in the data span are not troublesome, but the cumulative effect of the un-modeled thrusting in the prediction span produces secularly increasing uncertainties in the along-track direction.

Other findings were that position uncertainties at periapsis, important for science observations, tend to be smaller at lower periapsis altitudes. In addition, it was shown that ΔDOR data did dot significantly reduce OD uncertainties, so it will likely be used sparingly, if at all, during the mission orbital phase. The orientation of the orbit plane to the Earth line was not seen to have a large effect on estimation or propagation uncertainties. It also was found that OD errors during solar conjunction periods could increase by approximately 40% at the end of the prediction span. As expected, the prediction error associated with OCMs in the prediction span greatly increases the predicted position uncertainty. Several days of post-OCM tracking data will quickly determine the actual orbit. Particulars of the covariance analysis setup are given in Table 7.

Table 7. Pre-MOI Covariance Analysis Setup

Setup	**Notes**
Simulated Data	Operational schedule, approx. 12 hr/day

Data Type	**Data Weight**
2-Way Doppler	0.5 mm/s
2-Way Range	75 m

Estimated Parameters	**A-priori Uncertainty**
Spacecraft State	100 km, 50 m/s
Solar Pressure	Covariance, based on cruise phase
Commanded Momentum Dumps	1.4 mm/s
Mercury Gravitational Harmonics	From combined gravity field, thru flyby 3
Mercury Ephemeris	Covariance, DE423

Consider Parameters	**A-priori Uncertainty**
Station Locations	5×10^{-4}, 5×10^{-6}, 5×10^{-4} (0.5 m)
UT1 and Polar Motion	0.34×10^{-3}, 17×10^{-9} (15, 10 cm)
Troposphere (wet and dry)	1×10^{-2}, 4×10^{-2} (1, 4 cm)
Ionosphere	0.75, 0.15 (5, 1 cm)
Planetary Radiation Pressure	20×10^{-12} km/s^2
Earth Ephemeris	Covariance – DE423

The predicted uncertainties for a data cutoff of 13 April 2011 are shown in Figure 13. Figure 14 shows the predicted uncertainties, for a data cutoff of 14 June 2011, with OCM-1 in the propagation span and the fit span. Finally, Figure 15 shows the predicted uncertainties with and without ΔDOR.

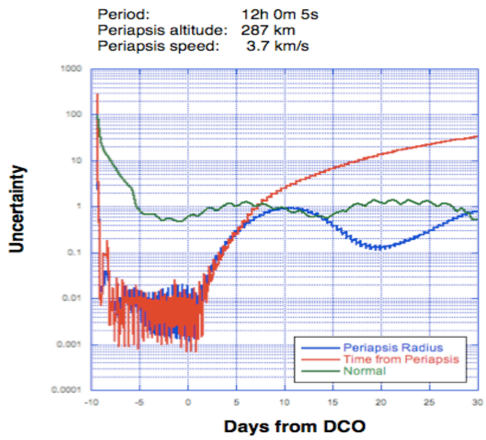

Maximum Errors (1-Sigma):

Days after DCO	R_p (km)	Δt (s)	N (km)
5	0.28	0.25	1
12	0.82	3.85	0.8
19	0.13	11.9	1.1
26	0.39	24.4	1

3-Sigma:

Days after DCO	R_p (km)	Δt (s)	N (km)
5	0.84	0.75	3
12	2.46	11.6	2.4
19	0.39	35.7	3.3
26	1.17	73.2	3

Figure 13. Predicted Uncertainties for a Data Cutoff of 13 April 2011. The Orbital Plane Is Perpendicular to the Earth Direction.

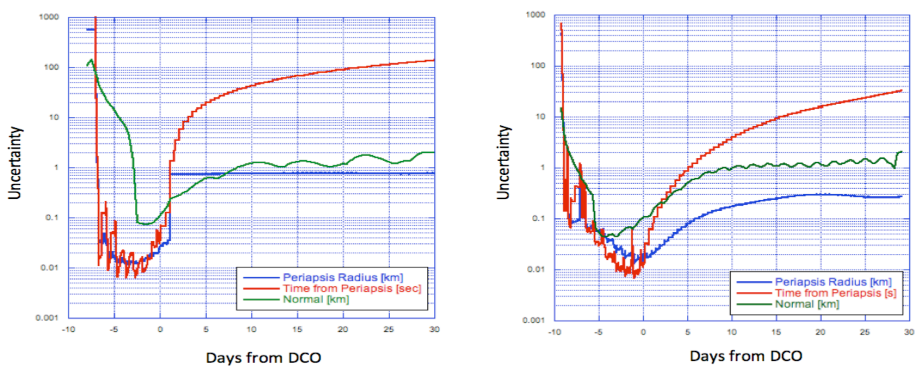

(a) OCM-1 in Propagation Span

(b) OCM-1 in Fit Span

Figure 14. Predicted Uncertainties For OCM-1 in (a) Propagation Span, (b) Fit Span.

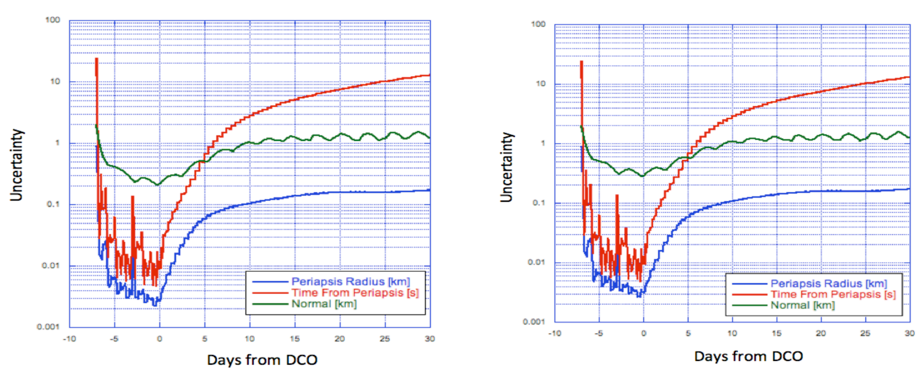

(a) Without ΔDOR

(b) With ΔDOR

Figure 15. Predicted RTN Uncertainties for a Data Cut Off of 23 October 2011 (a) without ΔDOR and (b) with ΔDOR.

Comparison of On-Orbit Predicted Trajectories

Science sequences for MESSENGER operations are normally planned three weeks in advance of execution. Therefore, accuracy of pointing, especially around periapsis, is very sensitive to errors in the predicted position in the direction of motion. Figure 16 shows comparisons of the predictions of the spacecraft along-track position for ODs 206 through 212 (operational ODs are numbered sequentially), expressed as periapsis crossing time, compared with subsequent best-estimate reconstructed values of the spacecraft position (i.e., compared with subsequent OD reconstructed trajectories). The timing error is determined by dividing the along-track position error by the instantaneous velocity magnitude. Position errors are defined as the difference between the predicted position of the spacecraft past the data cutoff for that particular OD solution, compared with the trajectory obtained from the fit-span portion of a subsequent OD solution. Smaller errors can be demonstrated for radial and out-of-plane errors. Figure 17 shows the error in periapsis passage time for ODs 206-212, after applying on-board time-tag biases. The latter are determined on the basis of subsequent OD solutions closer to the time of sequence execution and confirm that such errors can be greatly reduced to meet science objectives.

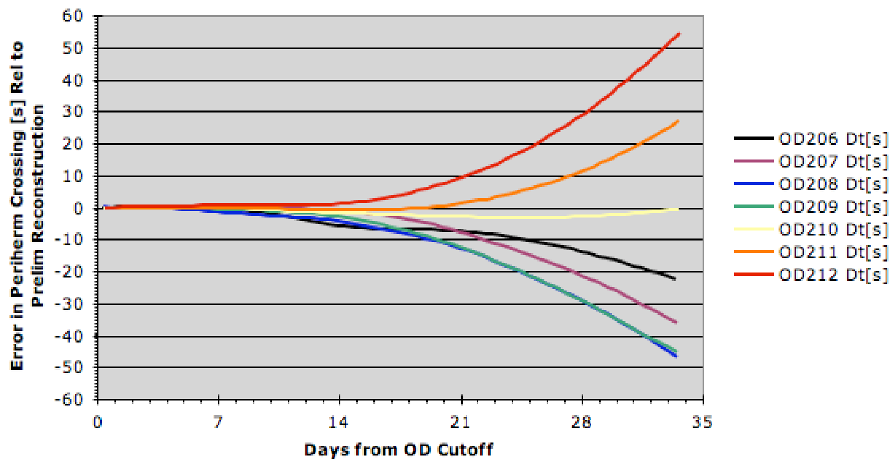

Figure 16. Example Prediction Errors for Periapsis Crossing Times.

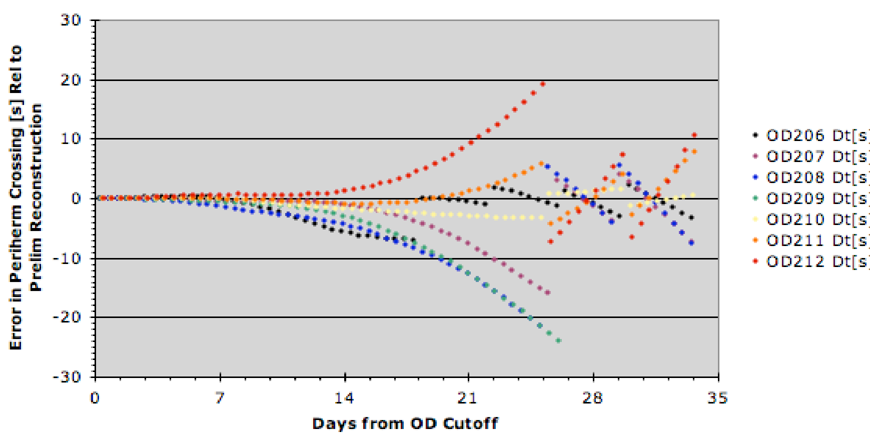

Figure 17. Example Prediction Errors for Periapsis Crossing Times, with On-Board Time-Tag Biases Applied.

As can be seen by comparing Figure 13 with Figure 16, the actual on-orbit errors are typically better than the 1-σ values predicted by the covariance analysis. For example, the timing bias in the table shown in Figure 13 predicts a 1-σ uncertainty of 24.4 s at 26 days from data cutoff. Figure 16 shows the actual value for OD's 208 and 209 to be about 23 s and the values for other ODs are also consistent with covariance estimates.

The covariance analysis showed that the primary driver of these uncertainties is the weekly momentum dumps. The navigation team cannot model these a priori, so trajectory predictions do not include future momentum dumps. If future momentum dumps could be predicted accurately in advance and included in the trajectory propagation, errors could be reduced. Unfortunately, accurate prediction of such small maneuvers is very difficult operationally.

Summary, Lessons Learned, and Future Plans

Several months and over one complete Mercury sidereal day have passed since MOI. Analysis of MESSENGER flyby data showed Mercury's ephemeris errors were very small (consistent with DE423 error covariances), and orbital data has led to further refinement in the Mercury ephemeris engineering models. A method has been implemented by the navigation team that combines information from separate data arcs to create a combined solution for the gravitational field. Engineering models generated using this technique have been used operationally and found to improve the quality and stability of the OD solutions. Ongoing experiments using a refined gravitational model, opening up the a priori uncertainties on the gravitational harmonics, are promising. Preliminary results indicate that the aliasing between the gravitational harmonics and the estimated radiation pressure parameters is significantly reduced. This outcome suggests that the gravitational harmonics are appropriately absorbing much of the force modeling uncertainty.

Separation of the planetary radiation pressure, solar radiation pressure, and higher-order gravitational harmonics continues to be a challenge for the navigation team. Additional analysis using improved gravitational models and correlating the solutions to Mercury-spacecraft-Sun geometry may help to separate the contributions from planetary radiation pressure and Mercury gravity. This work is ongoing and will improve as analysis continues through Mercury's second sidereal day and different geometries are encountered. There is currently no provision for thermal re-radiation from the spacecraft, modeled as 10 flat plates, which prevents fully optimal models from being generated. As was seen in the cruise phase, solar radiation pressure reflectivity coefficients varied while the overall trajectory prediction was quite good.[3] Aliasing between parameters determined in the solutions remains a challenge. However, the primary job of the navigation team is to provide an accurate predicted trajectory, and if the OD software trades off model parameters but still achieves this objective, that result is satisfactory operationally.

The ability operationally to upload an on-board time-tag bias mitigates the along-track prediction errors, which can be relatively large. These errors, due primarily to un-modeled commanded momentum dumps and systematic mismodeling of the spacecraft and planetary radiation pressure, are unavoidable as a priori knowledge of these perturbations is unavailable. Time-tag biases have enabled the project to compensate for this and still achieve the navigation and science objectives.

Trajectory reconstructions will be generated and distributed to the science and engineering teams by the end of the MESSENGER mission. Gravitational models updated as by-products of the reconstruction will be provided periodically. Collaboration with the MESSENGER science teams continues in order to continue to refine the gravitational models.

References

[1] Williams, B. G., A. H. Taylor, E. Carranza, J. K. Miller, D. R. Stanbridge, B. R. Page, D. Cotter, L. Efron, R. W. Farquhar, J. V. McAdams, and D. W. Dunham, "Early Navigation Results for NASA's MESSENGER Mission to Mercury," *Adv. Astronaut. Sci.*, 120 (Part II), 2005, pp. 1233-1250.

[2] McAdams, J. V., D. W. Dunham, R. W. Farquhar, A. H. Taylor, and B. G. Williams, "Trajectory Design and Maneuver Strategy for the MESSENGER Mission to Mercury," *J. Spacecraft Rockets*, 43 (5), 2006, pp. 1054-1064.

[3] Page, B.R., K.E. Williams, K.E., A. H. Taylor, A.H., D. R. Stanbridge, D. R., Bryan, C. G., Wolff, P. W., B.G. Williams, B. G., et al "Applying Experience From Mercury Encounters to MESSENGER'S Mercury Orbit Mission," *29th AAS/AIAA Space Flight Mechanics Conference*, paper AAS-549, Girdwood, AK, July 31-August 4, 2011.

[4] Margot, J. L., "A New Orientation Model for Mercury," *Celest. Mech. Dyn. Astron*., 105, 2009, pp. 329-336,

[5] Bierman, G. J., "Factorization Methods for Discrete Sequential Estimation", Academic Press, New York, 1977, 241 pp.

[6] Anderson, J. D., G. Colombo, P. B. Esposito, E. L. Lau, and G. B. Trager, "The Mass, Gravity Field, and Ephemeris of Mercury," *Icarus*, 71, 1987, pp. 337-349.

[7] Smith, D. E., M. T. Zuber, S. J. Peale, R. J. Phillips, and S. C. Solomon, "Estimating the Libration of Mercury by Remote Sensing of Gravity and Altimetry", Workshop Mercury: Space Environment, Surface, and Interior, Lunar and Planetary Institute, Houston, TX, 2001, pp. 90-91.

[8] Kaula W. M. (1966), "Theory of Satellite Geodesy," Blaisdell Publishing Co., Waltham, MA, p. 98.

[9] Borderies, N., and P. Longaretti, "A New Treatment of the Albedo Radiation Pressure in the Case of a Uniform Albedo and of a Spherical Satellite," *Celest. Mech. Dyn. Astron.*, 49, 1990, pp. 69-98.

[10] Borderies, N., "A General Model of the Planetary Radiation Pressure on a Satellite with a Complex Shape," *Celest. Mech. Dyn. Astron*., 49, 1990, pp. 99-110.

[11] BepiColumbo: An Interdisciplinary Cornerstone Mission to the Planet Mercury", System and Technology Study Report, ESA-SCI(2000)1, 2000.

[12] Leary, J. C. et. al., "The MESSENGER Spacecraft," Space Sci. Rev., 131, 2007, pp. 187-217.

[13] Thornton, C. L., and J. S. Border, "Radiometric Tracking Techniques for Deep-Space Navigation," Deep-Space Communications and Navigation Series, Monograph 1, Wiley-Interscience, Hoboken, NJ, 2003, pp. 47-58.

[14] Taylor, A. H., E. Carranza, J. K. Miller, D. R. Stanbridge, B. R. Page, J. Smith, P. Wolff, B. G. Williams, L. Efron, R. W. Farquhar, J. V. McAdams, and D. W. Dunham, "Earth to Venus Navigation Results for NASA's MESSENGER Mission to Mercury," *17th AAS/AIAA Space Flight Mechanics Conference*, paper AAS 07-171, Sedona, AZ, January 28-February 1, 2007, 20 pp.

[15] Williams, K. E., A. H. Taylor, B. R. Page, J. K. Miller, J. Smith, P. Wolff, D. R. Stanbridge, B. G. Williams, and J. V. McAdams, "Navigation for Second Venus Flyby of the MESSENGER Mission to Mercury," *18th AAS/AIAA Space Flight Mechanics Conference*, paper AAS 08-172, Galveston, TX, January 27-31, 2008, 20 pp.

[16] Dunne, J. A., and E. Burgess, "The Voyage of Mariner 10 Mission to Venus and Mercury," SP-424, NASA Scientific and Technical Information Office, Washington, DC, 1978.

[17] K. E. Williams, A. H. Taylor, D. R. Stanbridge, P. J. Wolff , B. R. Page, B. G. Williams, J. V. McAdams, "Navigation for the MESSENGER Mission's First Mercury Encounter," *2008 AIAA/AAS Astrodynamics Specialist Conference*, paper AIAA-2008-6761, Honolulu, HI, August 18-21, 2008, 20 pp.